Check for updates

RESEARCH ARTICLE

REVISED Optimisation of pipes with constant diameter using the heuristic optimality criterion

[version 2; peer review: 1 approved, 5 approved with reservations]

David Blacher[1], Michael Harasek[2]

[1]LKR Light Metals Technologies, AIT Austrian Institute of Technology, Lamprechtshausener Straße 61, Ranshofen, 5282, Austria
[2]Institute of Chemical, Environmental and Bioscience Engineering, TU Wien, Getreidemarkt 9/166, Vienna, 1060, Austria

v2 **First published:** 21 Sep 2023, **3**:156
https://doi.org/10.12688/openreseurope.15943.1
Latest published: 09 Apr 2026, **3**:156
https://doi.org/10.12688/openreseurope.15943.2

Abstract

Background

Minimising internal pressure drop in pipes is crucial for energy efficiency of fluid flow applications. Numerous computational optimisation tools that are capable of modifying flow geometries to reduce the pressure drop have been developed. Among these is a comparably simple heuristic optimisation al- gorithm which mimics erosion and sedimentation processes based on the shear stress in the vicinity of the domain boundaries. Although this method succeeds in modifying flow geometries for reduced pressure drop, it allows the fluid domain to widen during the reshaping process. Therefore, a reported reduction of pressure drop is not only caused by an improvement of the flow path, but also by an increase in the domain width. However, pipes with a constant circular diameter are favoured in many applications because they can be easily manufactured.

Methods

Here we combine the heuristic optimisation approach with a novel geometrical constraint that maintains constant average diameter throughout the reshaping process. To our knowledge, this is the first application of a diameter-preserving constraint to the heuristic optimality criterion, enabling assessment of pressure drop reduction achieved solely through flow path modification without diameter dilation effects. We determined the applicability of the new algorithm for 2D channel and 3D pipe ge- ometries, conducting numerical simulations using the Lattice Boltzmann method with Reynolds numbers ranging from 40 to 500.

Open Peer Review

Approval Status ? ? ? ✓ ? ?

	1	2	3	4	5	6
version 2 (revision) 09 Apr 2026				✓ view		? view
version 1 21 Sep 2023	? view	? view	? view	? view	? view	

1. **Sohail Rehman**, Islamia College Peshawar, Peshawar, Pakistan
2. **Somnath Roy**, Indian Institute of Technology Kharagpur, Kharagpur, India
3. **Hicham Ferroudji**, Boumerdes University, Boumerdes, Algeria
4. **Desejo Filipeson Sozinando**, Vaal University of Technology, Vanderbijlpark, South Africa
5. **S Mahmood Mousavi**, Seoul National University (Ringgold ID: 26725), Gwanak-gu, South Korea
Texas State University, San Marco, USA
6. **Sarmad A Ali**, University of Babylon, Babylon, Iraq

Any reports and responses or comments on the

Results

For the novel constant diameter constraint, the method successfully derived improved shapes across most tested Reynolds numbers while maintaining the initial average diameter. Notably, shapes derived at *Re* = 40 unexpectedly outperformed those derived at higher Reynolds numbers across all tested flow conditions, suggesting that low-Re geometries may capture fundamental flow features beneficial across wider Reynolds number ranges.

Conclusions

This finding suggests applicability to higher Reynolds number flows, potentially even at turbulent industrial flows to be investigated in future research.

article can be found at the end of the article.

Plain language summary

A high pressure drop in pipes limits the energy efficiency of machines, and there are computer tools that can change the pipe design to reduce the pressure drop. One method mimics erosion and sedimentation and is called heuristic optimality criterion. However, this method widens the pipe during the design process. This is problematic, because pipes with varying widths are harder to be produced. In this article, we describe how to restrict the reshaping method to leave the pipe width unchanged. We tested this method using computer simulations for 2D channels and 3D pipes with flows of different behaviours described by their Reynolds number. The Reynolds number describes the flow behaviour—whether it is smooth (laminar) or chaotic (turbulent). We successfully improved pipe shapes while keeping the diameter fixed across all tested conditions. Interestingly, we found that shapes designed for the lowest Reynolds number (Re=40) performed better than shapes specifically designed for higher Reynolds numbers. This unexpected result suggests that simple shapes derived at low flow speeds might work well across a wide range of conditions, potentially even for turbulent flows in industrial applications—an exciting direction for future research.

Keywords

Lattice Boltzmann method, shape optimization, heuristic optimality criterion, laminar internal fluid flow, pressure drop minimization, Cellular Automaton

H2020 This article is included in the Horizon 2020 gateway.

Corresponding author: David Blacher (david.blacher@ait.ac.at)

Author roles: Blacher D: Conceptualization, Data Curation, Formal Analysis, Investigation, Methodology, Project Administration, Software, Validation, Visualization, Writing – Original Draft Preparation, Writing – Review & Editing; **Harasek M**: Conceptualization, Project Administration, Supervision, Validation, Writing – Original Draft Preparation, Writing – Review & Editing

Competing interests: No competing interests were disclosed.

Grant information: The work presented here was conducted in the context of the Clean Sky 2 project COMBO3D. This project has received funding from the Clean Sky 2 Joint Undertaking under the European Union's Horizon 2020 research and innovation programme under grant agreement No 831851. This publication reflects only the authors' views and the European Union is not liable for any use that may be made of the information contained therein.
The funders had no role in study design, data collection and analysis, decision to publish, or preparation of the manuscript.

Copyright: © 2026 Blacher D and Harasek M. This is an open access article distributed under the terms of the Creative Commons Attribution License, which permits unrestricted use, distribution, and reproduction in any medium, provided the original work is properly cited.

How to cite this article: Blacher D and Harasek M. **Optimisation of pipes with constant diameter using the heuristic optimality criterion [version 2; peer review: 1 approved, 5 approved with reservations]** Open Research Europe 2026, **3**:156 https://doi.org/10.12688/openreseurope.15943.2

First published: 21 Sep 2023, **3**:156 https://doi.org/10.12688/openreseurope.15943.1

REVISED **Amendments from Version 1**

This revised version of our article incorporates significant improvements based on reviewer feedback.

The revised manuscript provides expanded methodological details including: convergence criteria based on kinetic energy monitoring, physical significance of boundary conditions, numerical parameter selection rationale, adaptation time justification, and fluid model description.

We have strengthened the presentation of our novel contribution: the first application of a diameter-preserving constraint to the heuristic optimality criterion. This innovation enables assessment of pressure drop reduction achieved solely through flow path modification, decoupled from diameter increase effects.

We have also put an emphasis on the significance of our finding that shapes derived at Re = 40 unexpectedly outperform those specifically optimized for higher Reynolds numbers (Re = 100-500) across all tested conditions. This suggests low-Reynolds-number geometries may capture fundamental flow features beneficial across wider Reynolds number ranges, potentially extending to turbulent industrial flows.

The manuscript now includes clearer physical context with real-world applications, a comprehensive future work section, and improved structural organization with a new validation section and enhanced conclusion.

Any further responses from the reviewers can be found at the end of the article

Table 1. Mathematical symbols frequently used. Bold letters represent vectors (e.g. $\boldsymbol{r}$). Capital letters with two subscript indices represent second-order tensors (e.g. S_{ij}), lower-case letters their elements (e.g. s_{ij}). Symbols with a tilde (e.g. $\tilde{t}$) denote dimensionless quantities.

Symbol	Unit	Meaning
Δp	1	Relative pressure drop
δt	1	Numerical time step
ρ	kg m^{-3}	Volumetric mass density
ξ_i	m s^{-1}	Particle velocity set of lattice model
d	m	Diameter
d_0	m	Initial diameter
f_e	1	Fraction of eroding nodes
f_s	1	Fraction of sedimenting nodes
t_a	t	Adaptation time
$f_i(\boldsymbol{r}, \xi, t)$	s^3 m^{-6}	Particle distribution function
M	1	Surface area in voxel units
p	N m^{-2}	Pressure
$\boldsymbol{r}$	m	Position
Re	1	Reynolds number
S_{ij}	s^{-1}	Strain rate tensor
$\|\|S_{i,j}\|\|$	s^{-2}	Frobenius norm of the strain rate tensor
u_0	m s^{-1}	Reference velocity
V	m^3	Fluid volume

1. Introduction

1.1 State of the art

Fluid flow applications such as heat exchangers, fluid distributors and gas ducts must be carefully designed to minimise pressure drop in order to maximise energy efficiency. Many approaches to optimise geometries exist, such as the adjoint[1,2] or conjugate gradient[3] method. These methods are capable of finding solutions for mathematical optimisation problems and allow for the combination of multiple objective- and cost-functions, making these approaches appropriate for a wide range of applications, including for turbulent flows[4] and the design of flow manifolds.[5] However, a geometry optimised in such a way might not always be feasible or economically viable because of practical, geometrical or material-

specific restrictions. Adding such constraints in a convenient mathematical form can be challenging and requires an experienced user with holistic knowledge about fluid dynamics, mathematical optimisation and the unique demands of the application. Wang et al.[6] proposed a different reshaping algorithm based on a relatively simple "heuristic optimality criterion". The shape of an initial flow geometry is modified in an iterative process: first, the fluid flow through the geometry is simulated using the Lattice Boltzmann Method (LBM). Then, the shape is slightly altered, mimicking erosion and sedimentation depending on the current flow field. These steps are repeated until a minimum pressure drop hence as optimum is found. The reshaping is governed by the following rules, implemented as a cellular automaton (CA):

- The fluid volume is kept constant throughout the reshaping process.
- The geometry only changes at the fluid-solid interface.
- Erosion occurs where viscous stress near wall nodes is highest. The neighbouring solid nodes become fluid.
- Sedimentation is applied to fluid nodes with the smallest value of dynamic pressure.

Wang et al. tested their method on 2D elbows and bifurcations and found a considerable reduction of pressure drop compared to the initial shapes across a range of Reynolds numbers from $Re = 0.0267$ to $Re = 80$. The applicability of the method was then proven by Wang et al. for the design of a fluid distributor.[7] Later, Tarlet et al. made use of the same method to derive a suitable geometry for a fluid mixer.[8] A similar approach was taken by Park et al.,[9] but they chose the strain rate as criterion for both erosion and sedimentation. Park et al. tested their method on 2D and 3D rectangular ducts at Reynolds numbers up to $Re = 100$. The resulting 2D elbow shapes are in close accordance with those Wang et al. published. Tao et al.[10] also implemented the heuristic optimality criterion but they combined it with additional optimisation approaches. They start with an empty box as initial fluid domain, within which an optimal flow can form unhindered by wall boundaries. Then, the fluid domain is shrunken by substituting fluid cells with solid zones where dynamic pressure is lowest until a certain volume is reached. During a second phase, the shape is further enhanced by erosion and sedimentation, with the volume being held constant similar to the heuristic optimality criterion as proposed by Wang et al. Unfortunately, Tao et al. did not specify how this volume was chosen in their publication, which is why a direct comparison of the results is non-trivial. Interestingly, Tao et al. adapted the method for ANSYS Fluent, a finite volume based solver. While the use of a finite volume based solver has some advantages over the Lattice Boltzmann Method (LBM see section subsection 2.1) such as fast convergence for steady-state simulations, it requires meshing of the fluid domain after each reshaping iteration. This time-consuming operation is not necessary when coupling a reshaping algorithm with the LBM.

1.2 Motivation - constant diameter constraint

The incompressible Navier-Stokes equations are simulated for a Newtonian fluid under isothermal conditions with isotropic, homogeneous and constant physical properties. This idealization is representative of many practical fluids such as water and air in moderate temperature ranges. Pipe elbow geometries are ubiquitous in fluid flow applications including heat exchangers, fluid distributors, and gas ducts in industrial systems, where pressure drop minimization directly impacts energy efficiency. The heuristic optimality criterion method was originally developed for laminar flows. This publication validates our implementation against the existing publications by Wang et al. and Park et al. before investigating the novel constant diameter constraint across Reynolds numbers from 40 to 500, which span the laminar flow regime.

While many industrial fluid flow applications—including air ducts, fluid distributors, and heat exchangers—operate in the turbulent regime at significantly higher Reynolds numbers, geometries derived for laminar flows may still provide performance benefits. Wang et al. successfully applied shapes derived at low Reynolds numbers to practical industrial applications operating at higher flow rates. Our findings show that shapes derived at $Re = 40$ unexpectedly outperform those derived at $Re = 100$–500 for their respective flow conditions (Section 4.4), suggesting that low-Re shape derivation may capture fundamental geometric features beneficial across a wider Reynolds number range—potentially extending into the turbulent regime. Investigating whether the constant diameter constraint enhances this transferability represents an interesting direction for future work.

The methods developed by Wang et al.,[6] Park et al.[9] and Tao et al.[10] offer simple ways to improve flow geometries. However, there is a major drawback limiting the applicability of the resulting geometries: in the presented cases, applying the reshaping algorithm results in a widening of the fluid domain diameter. This is because the path between inlet and outlet becomes shorter as the reshaping is applied. Due to the constant fluid volume constraint, the accumulating surplus of fluid nodes causes a widened cross section. This also implies that the reduction of pressure drop reported in the course

of the reshaping was not solely caused by an improvement of the flow path, but also by the increased domain width. Further increasing the width would likely cause the pressure drop to reduce even more. However, these geometries would not be favoured in real life applications where the diameter of pipes is often limited by a number of factors: available space, requirements regarding the stability of the pipes and material costs limit the possible size of the geometry. Moreover, the manufacturing process of pipes with varying diameter would require advanced techniques. Therefore, a new geometrical constraint is presented to counteract the diameter dilation. This novel constraint represents the key contribution of this work: unlike previous implementations by Wang et al., Park et al., and Tao et al., which allowed diameter variation, our method actively maintains constant average diameter. This decouples the pressure drop reduction due to flow path optimization from the trivial reduction achievable through diameter increase, enabling proper assessment when pipe diameter is constrained by space, structural requirements, or manufacturing considerations. We validate our implementation through numerical agreement with Wang et al. and Park et al. for a standard test case before investigating the constant diameter constraint. In the following, the Lattice Boltzmann Method (LBM) is briefly introduced. Then, the numerical setup is presented followed by a detailed description of the reshaping algorithm and the new reshaping constraint. The optimisation method was implemented as cellular automaton (CA) into the existing open-source LBM library called Palabos.[11]

2. Mathematical model

2.1 Lattice Boltzmann Method

An elaborate description of the lattice Boltzmann method (LBM) can be found for example in[12] on which this short introduction is based on. The LBM is a numerical model used for fluid flow simulations. It models the incompressible Navier-Stokes equations by solving a discretised Boltzmann transport equation, describing the evolution of the particle distribution function f_i due to particle interactions. The particle population f_i at each node $\boldsymbol{r}$ describes the number of particles moving with one velocity $\boldsymbol{\xi}_i$ out of a set of possible velocities. This set is designed in such a way that particles move from one node to a neighbouring node exactly within one numerical time step. For reasons of numerical stability and accuracy, a 3-dimensional model with 19 velocities (D3Q19) was used for all our test cases. The corresponding set of velocities $\boldsymbol{\xi}_i$ and their weights w_i of the D3Q19 lattice model are described by Figure 1 and Table 2. Aside from particles at rest ($i = 0$), all other velocities ($i \in [1, 18]$) point towards one of 18 neighbouring nodes. During one time step δt, the particles at each node $f_i(\boldsymbol{r})$ collide and then stream to neighbouring nodes:

$$f_i(\boldsymbol{r}+\boldsymbol{\xi}_i\delta t, t+\delta t) = f_i(\boldsymbol{r},t) + \Omega_i(\boldsymbol{r},t) \tag{1}$$

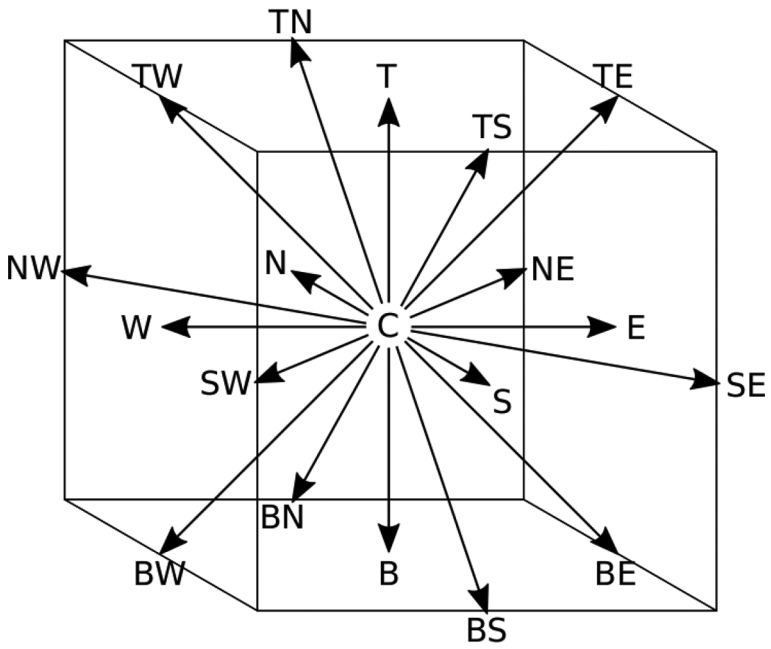

Figure 1. Discrete velocities of the D3Q19 lattice. To help visualise the phase space, each velocity is referred to by letters indicating its direction: "N,E,S,W,T,B,C" stand for "North, East, South, West, Top, Bottom, Center".

Table 2. Velocities ξ_i and weights w_i for the D3Q19 model. Velocities are scaled by the lattice velocity u_{lb}. The notation $(x, y, z)_c$ indicates all possible permutations of the given tuples.

ξ_i	w_i	$i \in$
(0, 0, 0)	1/3	{ C }
$(\pm u_{lb}, 0, 0)_c$	1/18	{ E, N, W, S, T, B }
$(\pm u_{lb}, \pm u_{lb}, 0)_c$	1/36	{ NE, NW, SE, SW, TE, TW, BE, BW, TN, TS, BN, BS }

For practical reasons, Equation 1 is separated in two computational steps. First the post-collision populations f_i^c are calculated at the current location $\boldsymbol{r}$:

$$f_i^c(\boldsymbol{r}, t+\delta t) = f_i(\boldsymbol{r}, t) - \frac{1}{\tau}(f_i - f_i^{eq}) \tag{2}$$

Then, the populations at ech node are updated based on the incoming particles from neighbouring nodes:

$$f_i(\boldsymbol{r} + \boldsymbol{\xi}_i \delta t, t+\delta t) = f_i^c(\boldsymbol{r}, t+\delta t) \tag{3}$$

In Equation 2, the post-collision particle interaction f_i^c is calculated by approximating the collision operator Ω as local relaxation towards equilibrium, the lattice Maxwell-Boltzmann distribution f_i^{eq}. This is known as the BGK model.

$$f_i^{eq}(\boldsymbol{r}) = \rho w_i \left[1 + \frac{1}{c_s^2}(\boldsymbol{\xi}_i \cdot \boldsymbol{u}) + \frac{1}{2c_s^4}(\boldsymbol{\xi}_i \cdot \boldsymbol{u})^2 - \frac{1}{2c_s^2}(\boldsymbol{u} \cdot \boldsymbol{u})\right] \tag{4}$$

The relaxation time τ depends on the chosen lattice viscosity ν_{lb}.

$$c_s = \frac{1}{\sqrt{3}} \quad \tau = \frac{\nu_{lb}}{c_s^2} + 1/2 \tag{5}$$

From the distribution function f_i, all relevant macroscopic flow properties can be calculated:

$$\rho = \sum_{i=0} f_i \quad p = c_s^2 \cdot \rho \tag{6}$$

$$\boldsymbol{u} = \frac{1}{\rho}\sum_{i=0}^{q} f_i \boldsymbol{\xi_i} \quad S_{ij} = -\frac{1}{2\tau c_s^2 \rho}\sum_{i=0}\left(f_i - f_i^{(eq)}\right)\boldsymbol{\xi_i}\boldsymbol{\xi_i} \tag{7}$$

The incompressible fluid is simulated under isothermal conditions, with isotropic, homogeneous and constant physical properties. The simulations conducted for this paper utilised regularised BGK dynamics, a multiple relaxation time (MRT) model. Latt et al.[13] showed that this enhanced model can reproduce analytically known solutions more accurately than the basic BGK model by restoring symmetry properties of the populations before every collision step. The LBM is particularly well-suited for shape optimization applications due to its natural handling of complex, evolving geometries without remeshing and straightforward implementation of boundary conditions on irregular surfaces. Table 3 lists the numerical parameters of the simulations for each chosen Reynolds number (Re). To ensure comparability with results by Wang et al. and Park et al., the resolution was set to the same value, given by the number of nodes across the

Table 3. Chosen numerical parameters given in lattice units. The maximum acceptable lattice viscosity ν_{lb}^{max} based on the Mach limit is provided for reference.

Re	Velocity u_{lb}	Viscosity ν_{lb}	$N_{cells,0} = 1/\delta_x$	ν_{lb}^{max}
40	0.04	0.04	40	0.0577
100	0.05	0.02	40	0.0231
200	0.05	0.01	40	0.0115
400	0.05	0.005	40	0.0058
500	0.05	0.004	40	0.0046

characteristic length (the inlet diameter) $N_{cells,0} = 1/\delta_x = 40$. This resolution choice prioritizes direct methodological comparison—enabling isolation of the constant diameter constraint effects—rather than grid convergence studies.

2.2 Numerical parameter selection

The choice of numerical parameters for LBM simulations requires careful consideration of several constraints to ensure stability and accuracy while maintaining computational efficiency. For a given Reynolds number *Re* and spatial resolution δ_x, the lattice viscosity v_{lb} must be chosen to satisfy the Mach number constraint, which requires flow velocities to remain well below the lattice speed of sound ($Ma = u_{lb}/c_s < 0.1$) for the incompressible LBM formulation.

Simulating a flow with a specific Reynolds number at a given resolution δ_x leaves the lattice viscosity v_{lb} as the only flexible parameter to ensure the Mach limit is not violated. The Mach limit imposes an upper bound on the acceptable lattice viscosity. Starting from the Mach number constraint and the definition of lattice viscosity, we derive:

$$Ma = \frac{u_{lb}}{c_s} = \frac{\delta_t}{\delta_x c_s} \leq Ma^{max} \tag{8}$$

$$\rightarrow \delta_t \leq Ma^{max} \delta_x c_s \tag{9}$$

Using the definition of lattice viscosity:

$$v_{lb} = \frac{\delta_t}{\delta_x^2 Re} \tag{10}$$

$$\rightarrow \delta_t = v_{lb} \delta_x^2 Re \tag{11}$$

Combining these expressions yields the maximum acceptable lattice viscosity:

$$\Rightarrow v_{lb} \leq \frac{Ma^{max} \cdot c_s}{\delta_x \cdot Re} = \frac{0.1}{\sqrt{3} \cdot \delta_x \cdot Re} \tag{12}$$

where $c_s = 1/\sqrt{3}$ is the lattice speed of sound for the D3Q19 model and $Ma^{max} = 0.1$. This relationship shows that higher Reynolds numbers require proportionally lower lattice viscosities to maintain numerical stability.

The relaxation time τ is related to the lattice viscosity through $\tau = v_{lb}/c_s^2 + 1/2$ and must satisfy $\tau > 0.5$ to ensure positive viscosity. Values of τ close to but above 0.5 can lead to numerical instabilities, while values significantly above 1 increase relaxation times. For the Reynolds numbers investigated ($Re = 40$ to 500), the chosen parameters (Table 3) maintain τ in a stable range while respecting the Mach limit.

The resolution of $N_{cells,0} = 40$ nodes across the inlet diameter was chosen to match Wang et al.[6] and Park et al.,[9] enabling direct methodological comparison. More detailed considerations regarding the overall research design, including convergence criteria and adaptation time selection, are provided in the accompanying thesis.[14]

2.3 Simulation setup

The initial pipe elbow geometry is created by two cylinders of the same diameter aligned perpendicularly to each other. One lies along the x-, the other along the y-axis. They extend from the inlet and outlet to the diagonal plane where they intersect. The simulation domain is a cuboid comprised of $N_{total} = N_x \cdot N_y \cdot N_z$ nodes. See Table 4 for the size of the domain for each geometry. The XY-plane at $z = N_z/2$ of the initial 3D elbow corresponds to the initial 2D elbow shape (see Figure 2). In the 2D simulations, a channel with infinite height is simulated by applying periodic boundary conditions in

Table 4. Optimisation parameters. Adaptation time between reshaping iterations $\tilde{t}_a$ is given as dimensionless value. The fraction of wall-neighbouring nodes subject to erosion in each iteration is denoted as f_e. The domain size consists of the total number of computational cells Nx,Ny,Nz.

	Optimisation		Domain size		
Type	$\tilde{t}_a$	f_e	**Nx**	**Ny**	**Nz**
2D channel	15	0.02	200	200	4
3D pipe	25	0.01	400	320	120

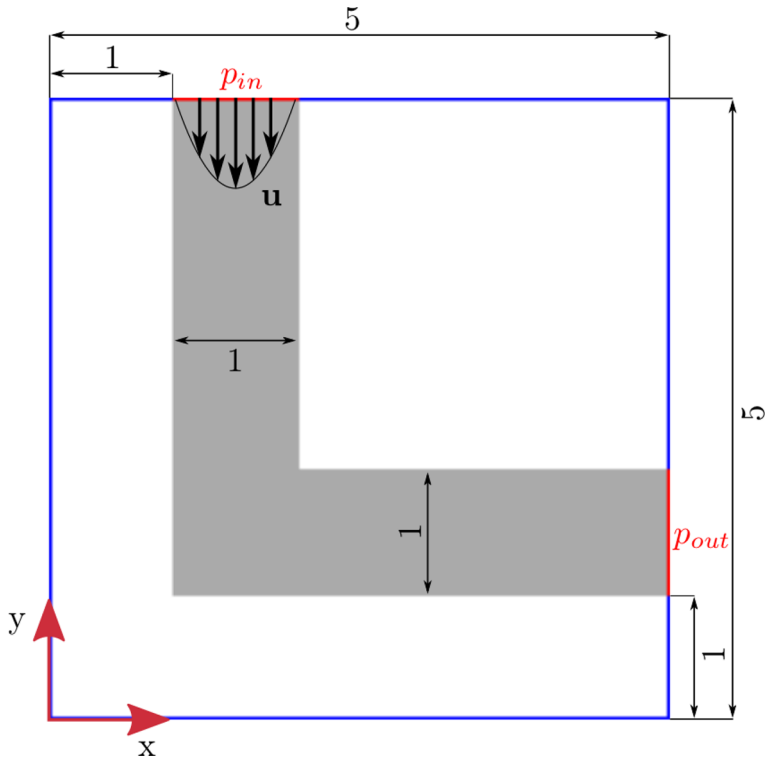

Figure 2. Initial 2D elbow geometry. Boundary conditions: prescribed velocity *u* at inlet; constant pressure at outlet. Red lines indicate where pressure is calculated for evaluation of pressure drop.

z-direction. At the outlet, a constant pressure condition $\tilde{p}_{out} = 1$ is imposed. This serves as a reference pressure (zero gauge pressure), allowing the flow to exit freely while enabling calculation of the pressure drop across the elbow geometry.

At the inlet, a parabolic velocity profile is imposed, representing a fully developed laminar flow condition characteristic of Poiseuille flow. This ensures the flow entering the elbow is representative of practical pipe flow conditions where flow has developed in an upstream section. The no-slip condition at solid walls is enforced through bounce-back dynamics, physically representing the zero velocity at the fluid-solid interface observed in viscous flows. Before the reshaping algorithm is applied, the flow field is initialised: starting from zero, the inlet velocity increases step-wise until it reaches the reference velocity $\tilde{u}_0 = 1$ in its centre. The flow is further simulated until the flow field converges to a steady state. Convergence is determined by monitoring the global change of kinetic energy—when this change falls below a specific threshold, the flow is considered to have reached steady state and reshaping may begin. This criterion ensures the initial flow field is fully developed before optimization starts. Between each reshaping iteration, the fluid flow is also simulated for an adaptation time $\tilde{t}_a$. This is necessary for the flow field to adapt to the modified geometry. Ideally, each reshaping step would be executed only after reaching a new steady state. However, this approach would require an impractical amount of computing time. Instead, a sufficient adaptation period was determined by analyzing the convergence of the wall shear stress distribution after a single reshaping step. This led to the choice of approximately 1.5 times the time needed for one flush through the geometry—long enough for the flow field to adapt adequately, yet computationally efficient. The chosen adaptation times for each geometry are listed in Table 4. This approach is more efficient than re-initializing the flow from zero velocity after each reshaping step, as done by Wang et al.[6] and Park et al.,[9] because the shape changes only incrementally between iterations.

3. Method

The individual steps of the optimisation procedure will be addressed in the following. As a reference, refer to Figure 5 which describes the implemented algorithm in a flowchart.

3.1 Erosion and sedimentation model

The reshaping algorithm allows modifications of the fluid domain only at the fluid-solid interface. Fluid nodes along the interface will be referred to as wall-neighbouring nodes in the remaining text. The reshaping is guided by a CA based on

the strain rate. To determine which of the wall-neighbouring nodes should be affected by the reshaping, they are ranked by the local value of $\|S_{i,j}\|$, the Frobenius norm of the strain rate tensor. Sedimentation will be applied to a fraction f_s of wall-neighbouring nodes where $\|S_{i,j}\|$ is smallest. Erosion will be applied to a fraction f_e of solid nodes directly neighbouring the fluid nodes which suffer from the greatest stress $\|S_{i,j}\|$. An eroding solid node joins the fluid domain by changing its dynamics from bounce-back to BGK. The resulting new fluid node is initialised with zero velocity, which is physically appropriate because these nodes are direct neighbors of solid walls subject to the no-slip condition. During the subsequent adaptation time $\tilde{t}_a$, the flow field adjusts to the new geometry and the initial zero velocity is replaced within a few time steps as the flow adapts. This simple initialization is both physically reasonable and computationally stable. If a fluid node sediments, it becomes a bounce-back node. In order to change the speed of the entire optimisation process, the fractions of affected nodes can be scaled: allowing more nodes to erode and to sediment in each step reduces the number of overall reshaping steps required to reach an optimised shape. However, Wang et al. recommend to choose a small fraction of affected nodes in order to ensure the shape actually converges to its optimum. Wang et al. chose the fraction of nodes affected by either erosion or sedimentation ($f_e + f_s$) as 0.04 of all wall-neighbouring interface nodes n_f. Park et al. varied the fraction between 0.02 and 0.05 in their simulations. The fractions of eroding nodes chosen for the present study is listed in Table 4. The ratio of eroding nodes to sedimenting nodes f_e/f_s determines if the fluid geometry may grow or shrink in each iteration. This balance is governed by the chosen reshaping constraint: either keeping the overall fluid volume or the geometry diameter constant throughout the reshaping. In order to keep the fluid volume constant, the total number of fluid nodes must not change, requiring $f_e/f_s = 1$ throughout the entire optimisation process. A constant geometry diameter can be achieved by adjusting the ratio of eroding nodes to sedimenting nodes during the reshaping process.

3.2 Calculation of current diameter

The fluid volume V is calculated as the sum of all fluid nodes:

$$V = n_{fluid} \cdot V_n = n_{fluid} \tag{13}$$

where n_{fluid} is the number of fluid nodes and $V_n = 1$ is the volume per node in lattice units.

At each iteration, the diameter is evaluated by considering the relationship between volume and surface area of the fluid domain. This is based on a generalisation of the theorem of Pappus,[15] which allows the calculation of surface area and volume for a solid generated by moving a plane figure F (enclosed by curve C) perpendicularly along an arbitrary curve L. Figure 3 depicts how both the initial and an exemplary optimised pipe geometry can be described as such a solid. Its volume V equals the product of the area A of figure F and distance l_F travelled by the centroid of F:

$$V = A \cdot l_F \tag{14}$$

Provided the traced curve L lies in a plane, the generated body's surface area M equals the product of the arc length s of C and the distance l_C travelled by the geometric centroid of C:

$$M = s \cdot l_C \tag{15}$$

Consequently, we can write the ratio of a body's volume to its surface area as:

$$V/M = \frac{A \cdot l_F}{s \cdot l_C} \tag{16}$$

For the simple cases of figure F being either a circle or rectangle, the centroids of figure F and curve C coincide, and $l_F = l_C = l$, resulting in:

$$\Rightarrow V/M = \frac{A}{s} \tag{17}$$

For a circle with radius $r = d/2$ we get:

$$V/M_{\bigcirc} = \frac{r^2\pi}{2\pi r} = \frac{r}{2} = \frac{d}{4} \tag{18}$$

This corresponds to a pipe with circular cross section. A channel with infinite height (quasi 2D case) can be approximated as a slender ($h >> d$) rectangle with width d and height h:

$$V/M_{\bigcirc} = \frac{dh}{2(d+h)} = \frac{d}{2\left(\frac{d}{h}+1\right)} \approx \frac{d}{2} \tag{19}$$

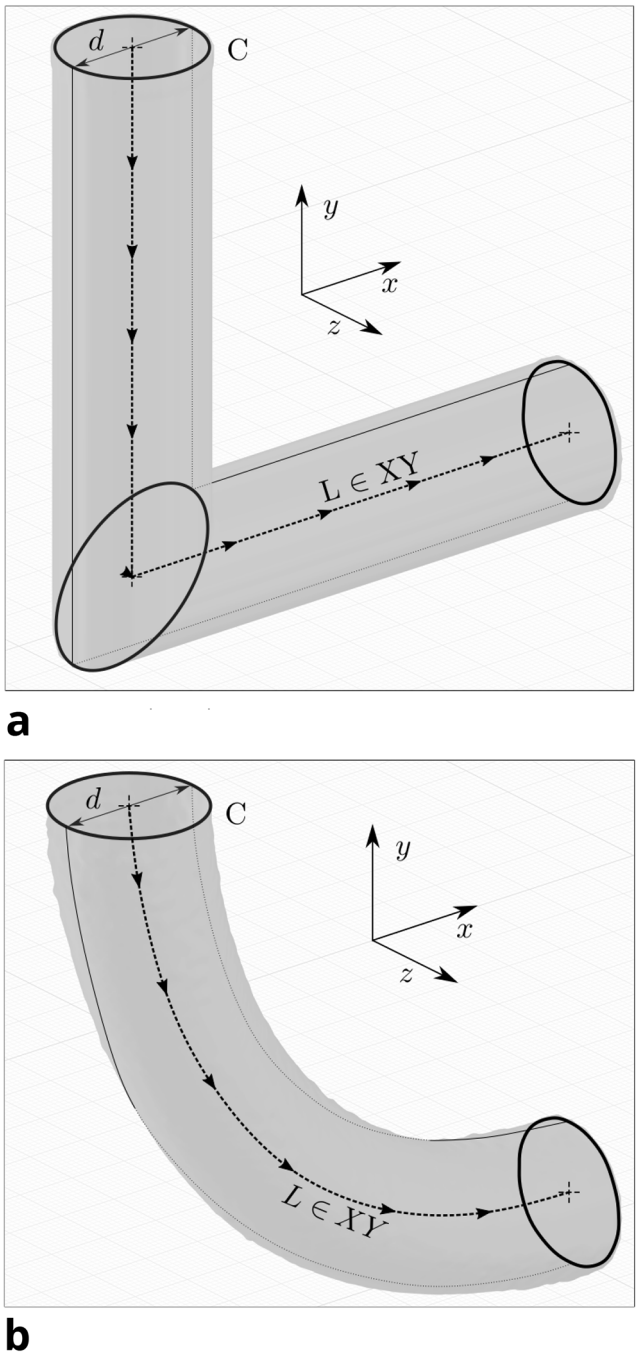

Figure 3. Geometrical analysis: by tracing figure F (enclosed by curve C) along the path L (which lies in the XY-plane), the 3D pipe geometry can be generated. (a) Initial geometry. Curve C is depicted 3 times: at the inlet, the intersection of cylinders and at the outlet. (b) Optimised geometry for *Re* = 40. Curve C is depicted 2 times: at the inlet and outlet.

In both cases, the ratio V/M is proportional to the diameter d, but independent of the curve. Therefore, the average diameter of these geometries can be gauged by V/M even if the path l changes. This calculation method is not suited for complex geometries, such as bifurcations or 3D geometries with non-circular cross sections. For the conducted simulations, the change of the diameter relative to its initial value d/d_0 was of interest. This ratio can be calculated with knowledge of the initial values of volume V_0 and surface area M_0 and their current values V and M:

$$\frac{V/M}{V_0/M_0} = \frac{d}{d_0} = \frac{\tilde{d}}{\tilde{d}_0} \tag{20}$$

In dimensionless values the initial diameter $\tilde{d}_0$ is 1, and the current diameter is calculated as

$$\rightarrow \tilde{d} = \frac{V/M}{V_0/M_0} \tag{21}$$

The volume V is approximated by the sum of all fluid nodes, with a volume of $V_n = 1$ each: The surface area M is calculated from a generated smoothed STL representation of the fluid-solid interface.[16] The STL file format is commonly used to store a 3D representation of a surface comprised of unstructured triangulated sub-surfaces, each defined by its unit normal and vertices.

3.3 Adjusting the erosion/sedimentation ratio for a constant diameter

The measurement of the diameter allows to adjust the erosion/sedimentation ratio to counteract shrinking or widening during the reshaping process. Each reshaping step consists of the erosion process, a re-evaluation of the diameter and, if necessary, one or more layers of sedimentation. Sedimentation is applied incrementally until the diameter reaches its initial value. The number of sedimenting nodes for each increment is proportional to the current deviation of the diameter from its initial value:

$$f_s = \left(\frac{d}{d_0}\right)^3 - 1 \quad \text{for 3D pipe} \tag{22}$$

$$f_s = \left(\frac{d}{d_0}\right)^2 - 1 \quad \text{for 2D channel} \tag{23}$$

This ensures convergence of the diameter to its initial value. In order to allow regions with little fluid flow to sediment first, a new layer of solid nodes can be added on top of the last with each increment. Because the fluid-solid interface changes each time, a new ranking by local strain rate $\|S_{i,j}\|$ is required to determine the nodes for the next increment. However, as no fluid flow is simulated between these incremental sedimentation steps, the ranking of the new wall-neighbouring nodes is based on strain rate information of the previous reshaping step. Figure 4 shows how the initial hard edge of the elbow geometry becomes rounded during the first reshaping step. Such a sedimentation of multiple layers occurs mainly in the first few reshaping steps.

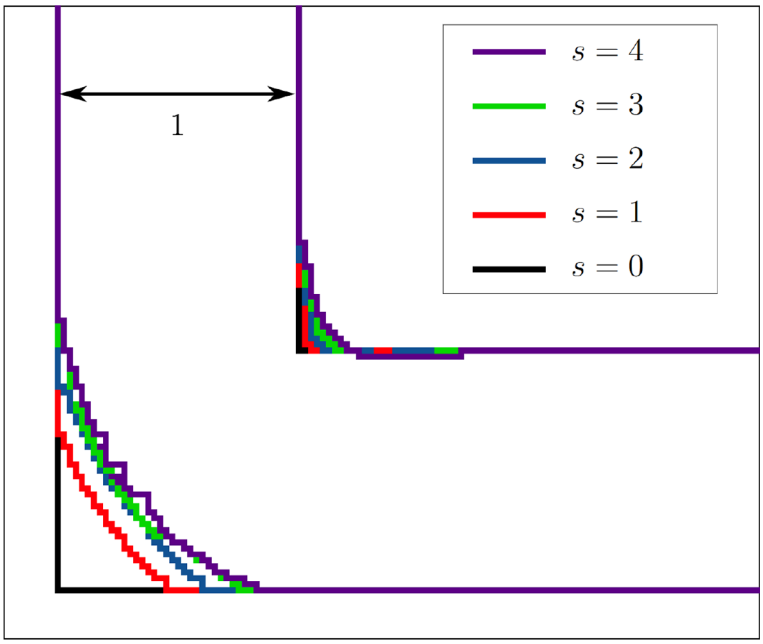

Figure 4. Reshaping of the 2D elbow channel. During the first two reshaping steps, multiple layers sediment. In the subsequent steps, only few multi-layer sedimentation steps take place.

3.4 Pressure drop evaluation

The inlet pressure $\tilde{p}_{in}$ was calculated as the average at the inlet domain boundary. The outlet pressure is defined as the reference pressure $\tilde{p}_{out} = 1$. The dimensionless absolute pressure drop $\Delta\tilde{p}_a$ of a given fluid flow is the difference between inlet and outlet:

$$\Delta\tilde{p}_a = \tilde{p}_{in} - \tilde{p}_{out} = \tilde{p}_{in} - 1 \tag{24}$$

To allow the comparison of the pressure drop reduction in simulations with different Reynolds numbers, the relative pressure drop was calculated. The relative pressure drop for a given shape is the ratio of its current absolute pressure drop and the absolute pressure drop of the initial elbow shape.

$$\Delta p = \frac{\Delta\tilde{p}_a}{\Delta\tilde{p}_{a,init}} \tag{25}$$

By this definition, the optimisation of any shape started at a relative pressure drop of Δp = 1. If the pressure drop continuously increased after hitting a minimum or the shape converged to a final shape, the simulation was terminated and the shape yielding the best result exported.

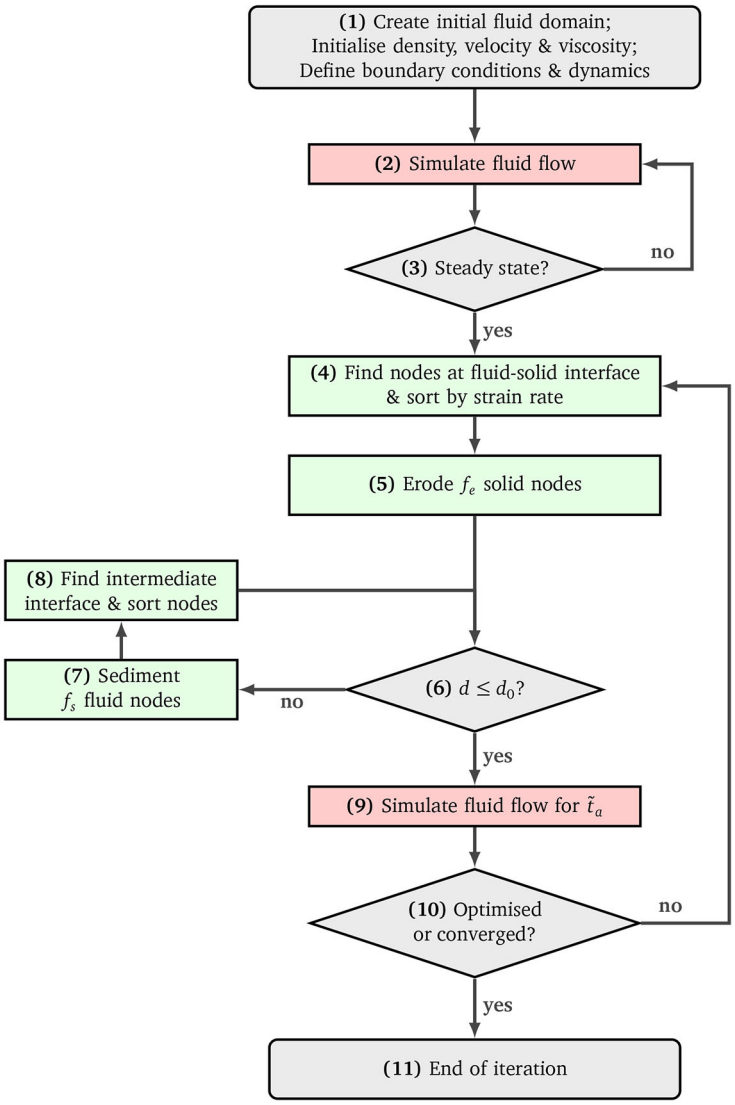

Figure 5. Flowchart of the reshaping algorithm.

4. Results and discussion

4.1 Validation against literature

To validate the implementation of the heuristic optimality criterion, the 2D channel elbow was optimized at $Re = 40$ under the constant volume constraint using identical numerical parameters as Wang et al.[6] and Park et al.[9]

Figure 6 compares the optimized shapes. Our method achieved a pressure drop reduction to $\Delta p_{opt} = 0.322$ (67.8% of the initial value), in excellent agreement with Wang et al. (68.8%) and Park et al. (66%). This close numerical agreement across three independent implementations confirms the correct application of the heuristic optimality criterion and validates the LBM simulation approach. This established baseline enables confident investigation of the novel constant diameter constraint introduced in this work.

The agreement also demonstrates that our choice of adaptation time and velocity initialization approach produces results consistent with the original methods, despite using a different flow field update strategy between reshaping steps.

Table 5 summarises the pressure drop achieved during the reshaping process. For all tested setups, shapes derived under the constant volume constraint yielded a smaller pressure drop at a wider diameter.

4.2 2D channel elbow

As validated in Section 4.1, our implementation produces results in excellent agreement with Wang et al. and Park et al. for the constant volume constraint. We now investigate the novel constant diameter constraint.

Figure 8 visualises the change in pressure drop over the course of the reshaping for both constraints. In simulations with higher Reynolds numbers, an even smaller of Δp_{opt} could be achieved. Figure 7 shows that the curvature of the resulting shapes increases with rising Reynolds number. This behaviour was also reported by Wang et al. across a range of lower Reynolds numbers. They found a straight connection between inlet and outlet for $Re = 0.0267$, and arc like shapes at $Re = 20, 40, 80$. In all but one of the simulations, the pressure drop converges to a minimum. Only during the optimisation at $Re = 40$ under the constant diameter constraint, Δp_{opt} increased again by 2.6% after reaching a minimum at $s = 379$ reshaping steps. The evolution of shape during this simulation is depicted in Figure 9a. In all other 2D simulations, the geometry had reached a final shape and Δp_{opt} its final value after approximately $s = 500$ reshaping iterations. The evolution of shape during one such simulation is depicted in Figure 9b. At $s = 1000$ reshaping iterations, the simulations were terminated.

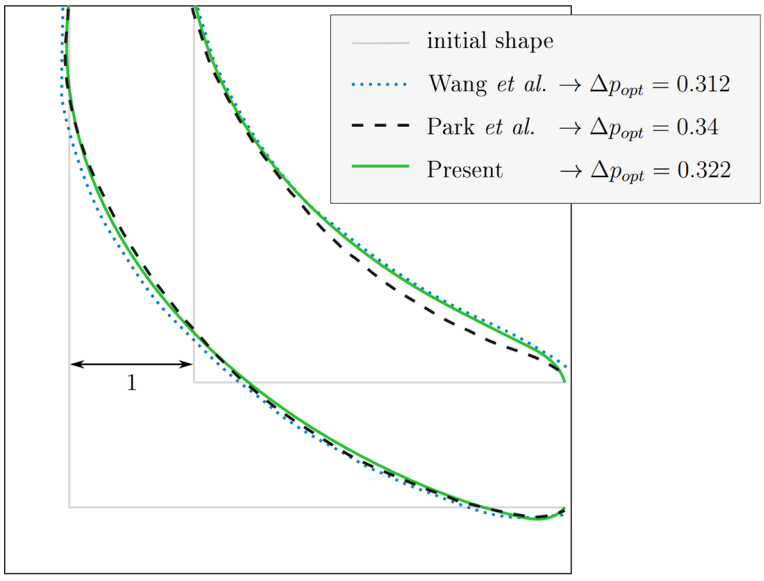

Figure 6. 2D elbow: optimised shape at $Re = 40$ for constant volume. Comparison with existing publications.[6,9] Our result is depicted here and in Figure 7a as solid green line.

Table 5. Results of conducted simulations: Setup parameters are listed on the left hand side. On the right hand side, information on the optimised shape are given. Optimised pressure drop Δp_{opt} and diameter d are relative to values at initial elbow shape. The number of the reshaping steps after which a minimum pressure drop was reached is listed as s_{opt}. A '+' symbol indicates that the shape was fully converged at this step.

Geometry	Constraint	*Re*	Δp_{opt}	*d*	s_{opt}	
2D channel	V	40	0.322	1.287	960	+
	V	200	0.130	1.240	605	+
	V	500	0.036	1.230	619	+
	d	40	0.739	1.001	379	
	d	200	0.472	1.002	771	+
	d	500	0.255	1.002	652	+
3D pipe	d	40	0.902	1.000	658	+
	d	100	0.972	1.000	125	
	d	200	0.943	1.000	38	
	d	400	0.832	1.000	147	

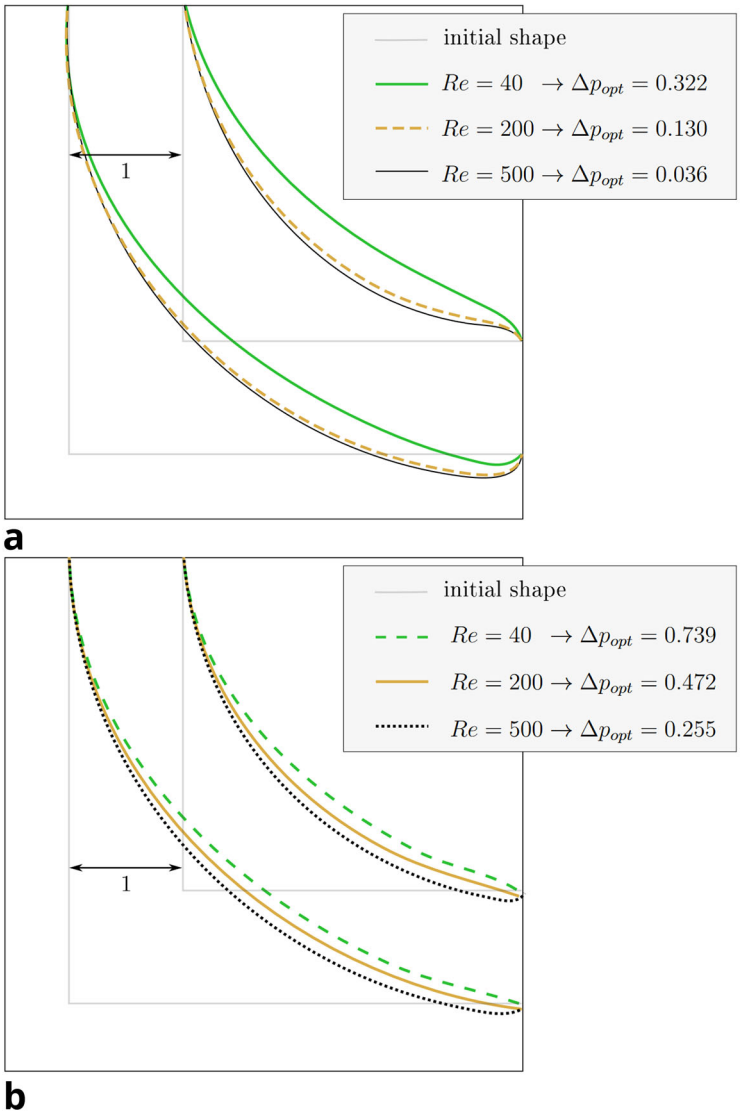

Figure 7. 2D elbow: optimised shapes. (a) Shapes derived under constant volume constraint. (b) Shapes derived under constant diameter constraint.

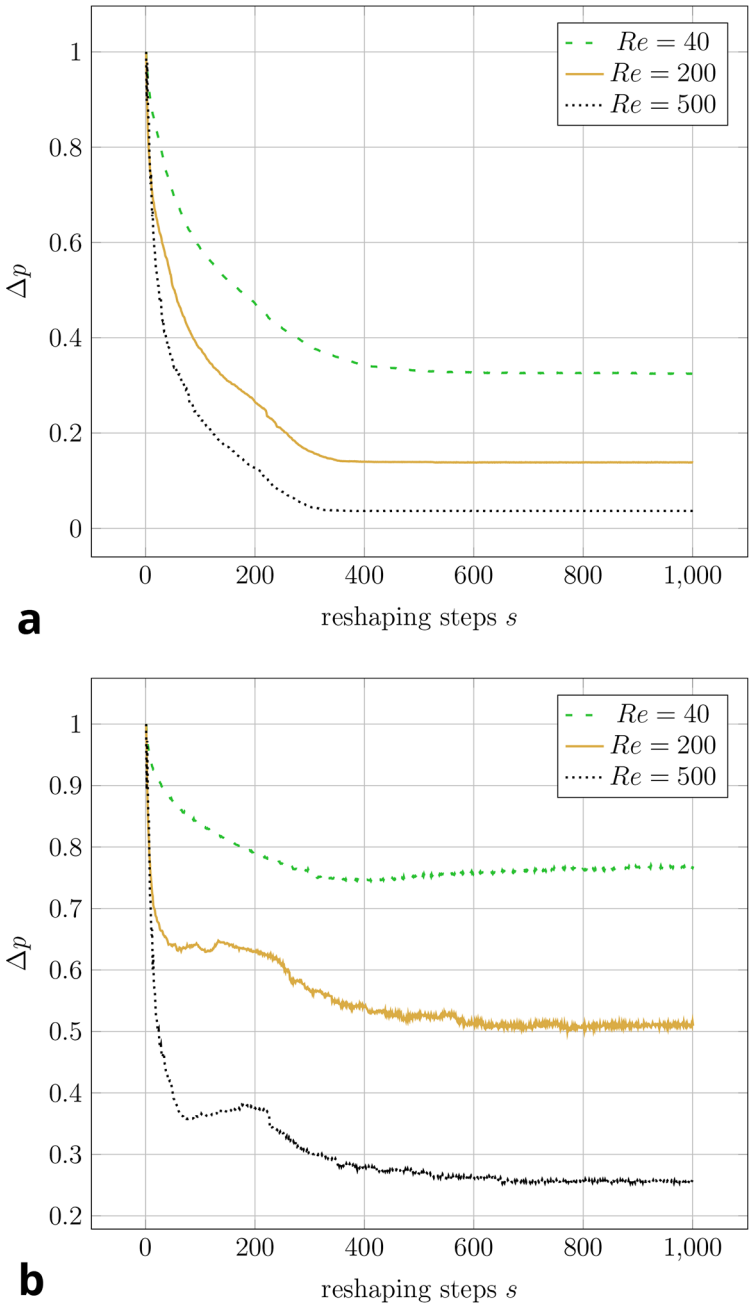

Figure 8. 2D elbow: Evolution of relative pressure during the reshaping (at varying Reynolds numbers at either of the two reshaping constraints). For each simulation, the pressure drop values are relative to their initial values. Simulations at the same Reynolds number start with the same absolute pressure drop (the difference between inlet and outlet). (a) Constant volume constraint. (b) Constant diameter constraint.

4.3 3D pipe elbow

For the 3D pipe geometry, only reshaping with the constant diameter constraint was performed. Interestingly, the achieved relative pressure drop does not follow a clear trend. Figure 13 shows that Δp only converges to a minimum during the reshaping at $Re = 40$. To eliminate the influence of potential spatial limitations, a longer outlet was simulated by doubling the domain in the x-direction. 3D renderings of the derived shapes for $Re = 100$ and $Re = 400$ are visible in

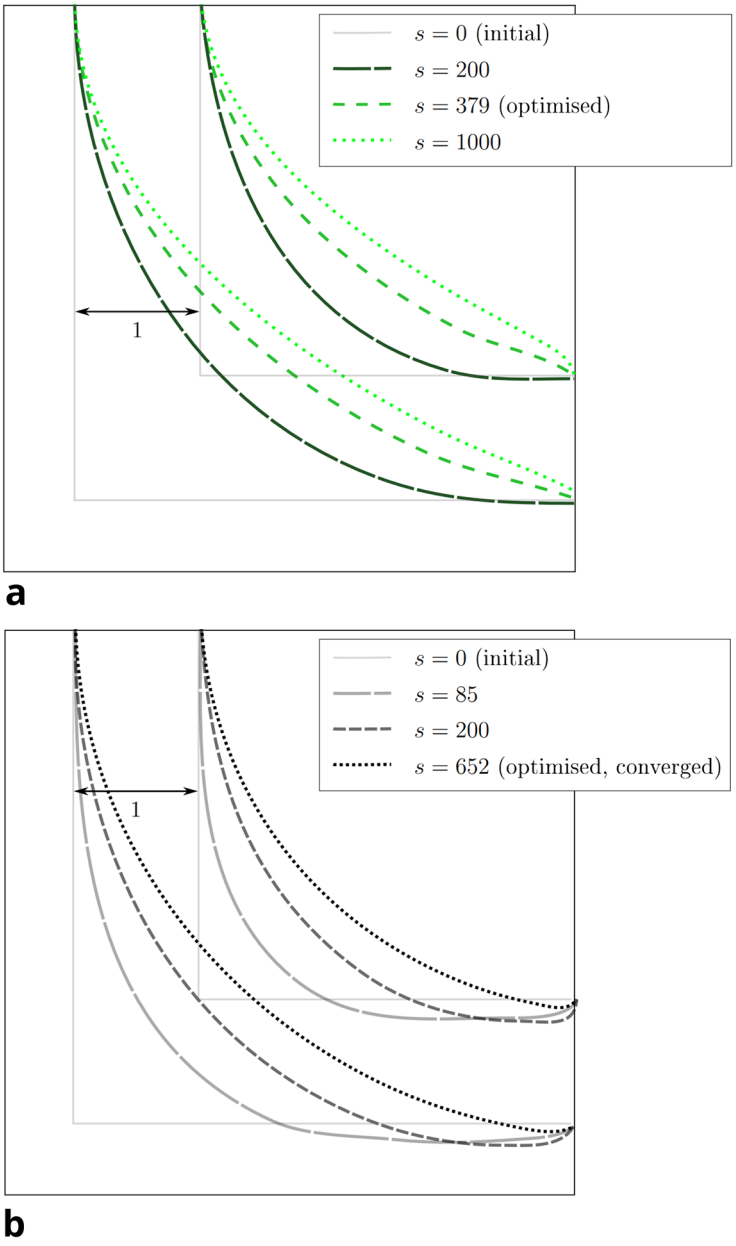

Figure 9. 2D elbow: snapshots taken at selected reshaping steps *s* during reshaping. (a) Evolution of shape at *Re* = 40 and constant diameter. (b) Evolution of shape at *Re* = 500 and constant diameter.

Figure 10. The shape derived at *Re* = 40 closely resembles those found in 2D at this Reynolds number (see Figure 11a): inlet and outlet are connected by an arc like shape. However, the shapes derived at *Re* 100 behave differently: the elbow dips below the level of the outlet, as visible in Figure 12a. Furthermore, the pipe cross section deviates from a circular profile: Figure 11b shows that for *Re* = 40, the cross section is still close to a circular profile. Above that, deviations increase with the Reynolds number, as visible in Figure 12b. The shear stress fields of the flow at *Re* = 200 in the initial and optimised 3D pipe are plotted in Figure 14 and Figure 15.

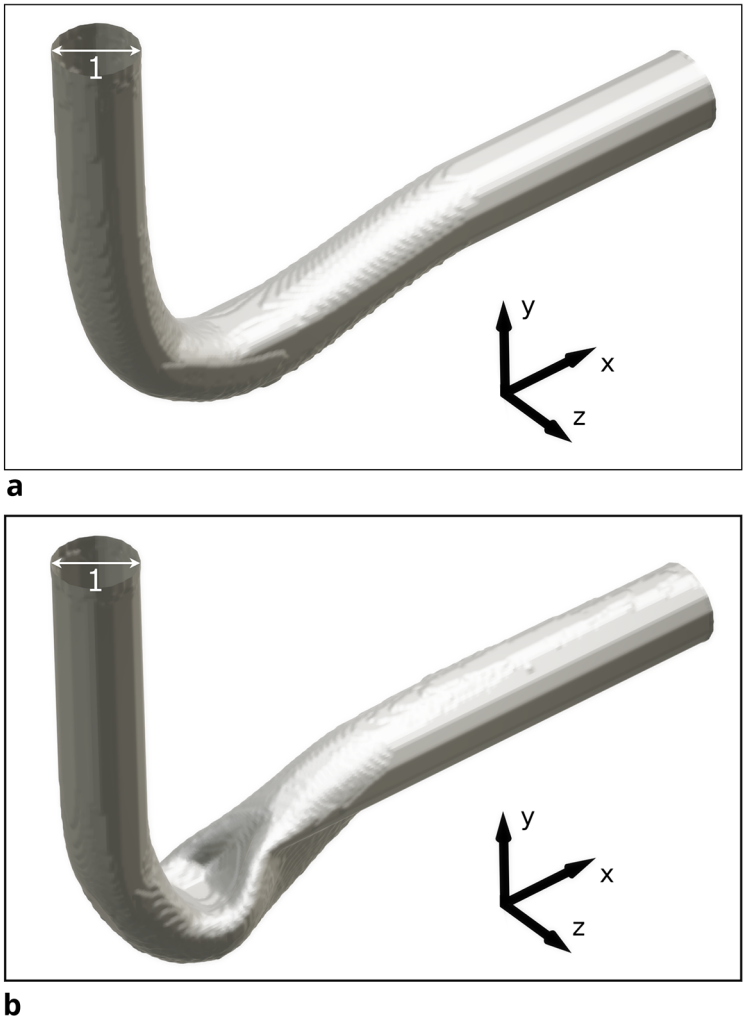

Figure 10. 3D visualisation of pipe optimised at two Reynolds numbers. (a) $Re = 100$. (b) $Re = 400$. The pipe shows significant deformation.

4.4 Convergence of shapes

For this study, the direct dependence of the shape optimisation on a variation of the initial geometry was not investigated, but some conclusions can still be drawn from the observed convergence behaviour. In any 3D simulation with $Re \geq 100$, the shapes did not converge to reach a minimum pressure drop. Instead, an intermediate iteration with a minimum pressure drop could be identified by the algorithm. This is visible in Figure 13. Consequently, the intermediate shape with the lowest pressure drop could not have been returned if a subsequent iteration of the reshaping had been used as the initial shape. Therefore, there seems to be a dependency of the optimisation algorithm on the initial geometry for 3D geometries at $Re \geq 100$ which demands to be explored in more detail. While Wang et al.[6] reported that the optimisation of 2D shapes at $Re = 40$ was largely unaffected by the initial geometry, this could not be verified for the reshaping with the new constant diameter constraint at $Re = 40$: here the smallest pressure drop was found after $s = 379$ iterations (see Table 5 and Figure 9a). For all other 2D cases, the geometry converged to a minimum. Overall, this indicates that the algorithm is indeed dependent on the starting geometry.

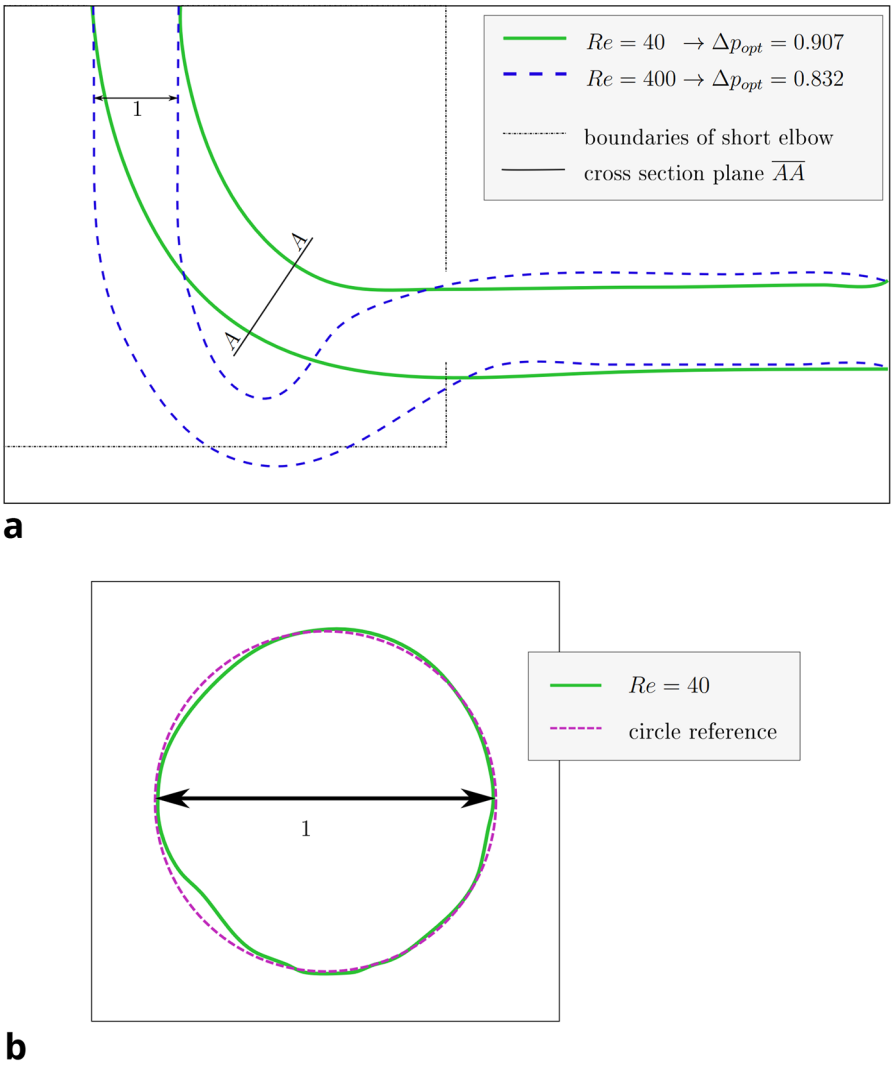

Figure 11. 3D elbow: projections of shape derived at *Re* = 40. (a) XY-plane projection of shape derived at *Re* = 40. The cross section in plane $\overline{AA}$ is depicted in figure b. The shape optimised at *Re* = 400 and the domain boundaries of the shorter 2D elbow are depicted for reference. (b) The cross section (plane $\overline{AA}$) of the shape derived at *Re* = 40 retains an almost circular profile.

4.5 Quality of derived shapes

For both constraints and all setups (2D and 3D), shapes could be derived which yielded a reduced pressure drop compared to the initial geometries. The shapes derived at $Re = 40$ exhibit the shortest connection between in- and outlet. To rule out that these shapes perform better than the longer connections derived at $Re \geq 100$, additional flow simulations were performed: for each tested Reynolds number $Re \geq 100$, the flow through the reference shape derived at $Re = 40$ was analysed and $\Delta p_{Re=40}$ calculated. The values are summarised in Table 6. Surprisingly, the reference shape derived at $Re = 40$ resulted in the lowest pressure drop for flows, across all tested Reynolds numbers. This behaviour was found both among the shapes derived with the constant diameter and the constant volume constraint. These findings indicate that the algorithm as adapted from Wang et al. and Park et al. encounters difficulty finding Reynolds-number-specific optima at $Re \geq 100$. However, the superior performance of the $Re = 40$ shapes across all tested Reynolds numbers suggests an intriguing possibility: shapes derived using the heuristic optimality criterion at low Reynolds numbers may

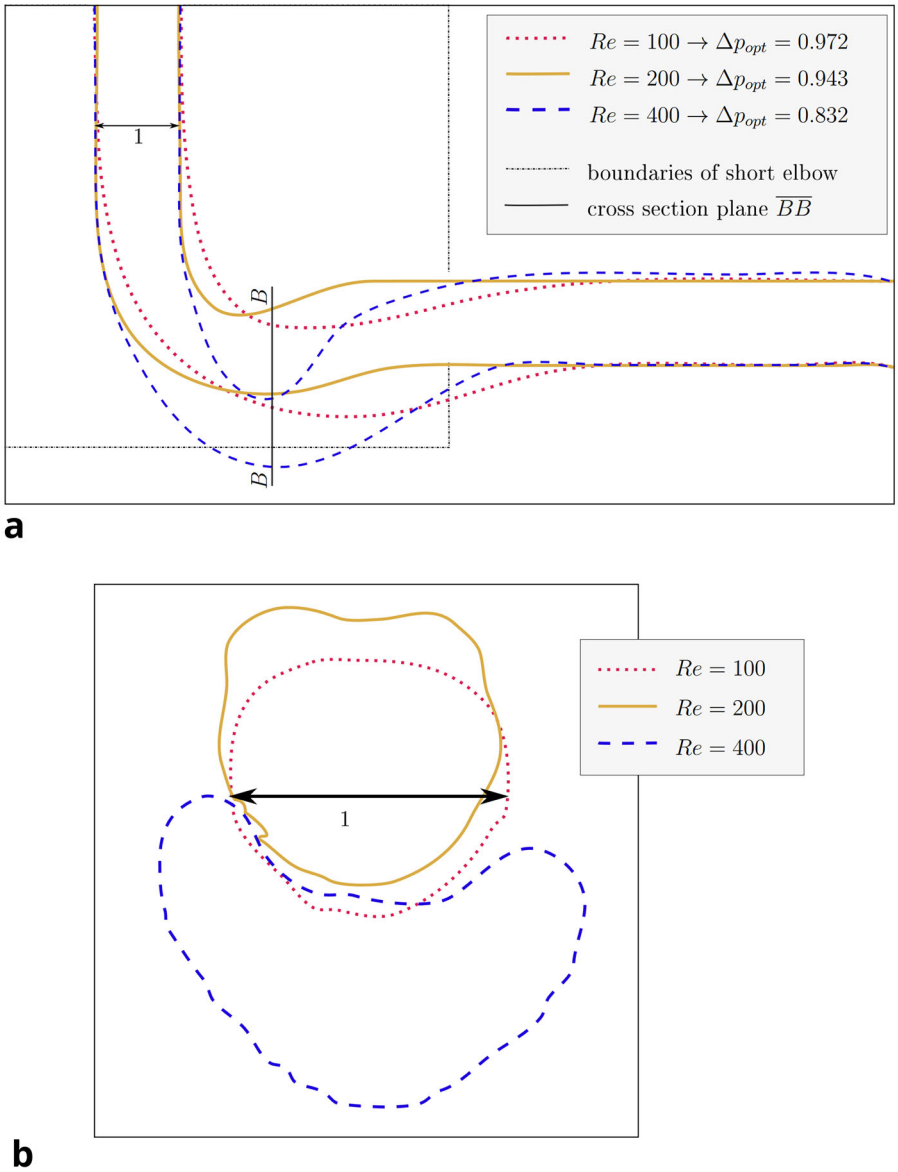

Figure 12. 3D elbow: projections of shapes derived at *Re* ≥ 100. (a) XY-plane projection of shapes. The cross section in plane $\overline{BB}$ is depicted in figure (b). The domain boundaries of the shorter 2D elbow are depicted for reference. (b) The cross sections of shapes in plane $\overline{BB}$ (corresponds to YZ-plane at $\tilde{x} = 3$, equivalent to $n_x = 120$). With increasing Reynolds number, the deviation from a circular profile becomes more pronounced.

capture fundamental flow path features that remain beneficial at higher Reynolds numbers. If this transferability extends to turbulent flows—as Wang et al. demonstrated in practical applications—the heuristic optimality criterion combined with the constant diameter constraint could offer a computationally efficient approach to derive geometries applicable across a wide Reynolds number range, including turbulent industrial conditions. This hypothesis warrants investigation in future work.

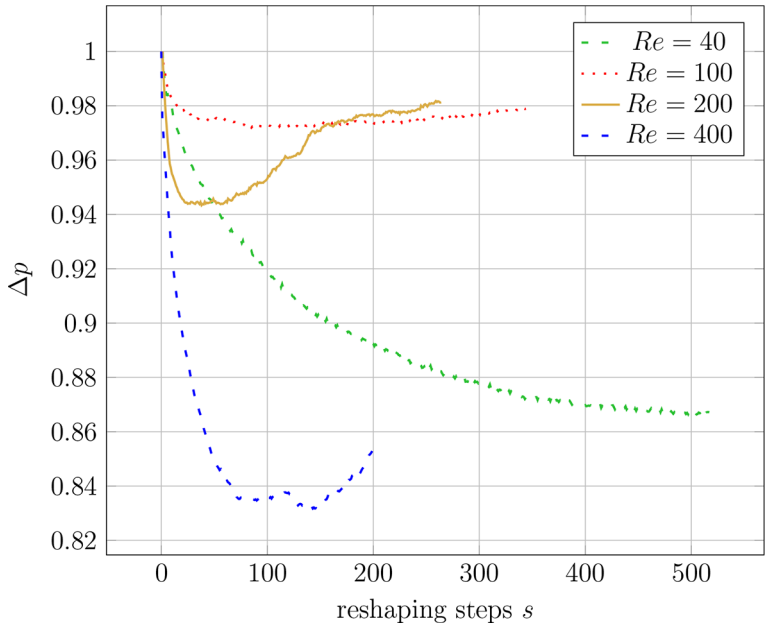

Figure 13. 3D elbow: evolution of relative pressure drop during reshaping at different Reynolds numbers.

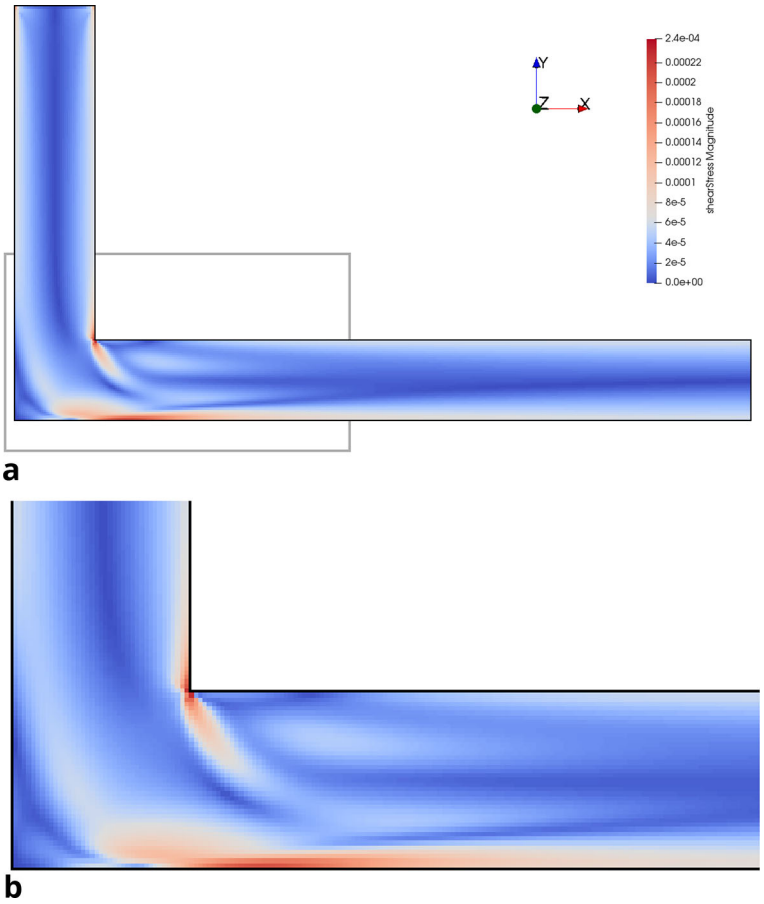

Figure 14. Shear stress in initial 3D pipe elbow at *Re* = 200. (a) Full geometry. Grey box indicates area of detailed view in figure below. (b) Detail of geometry.

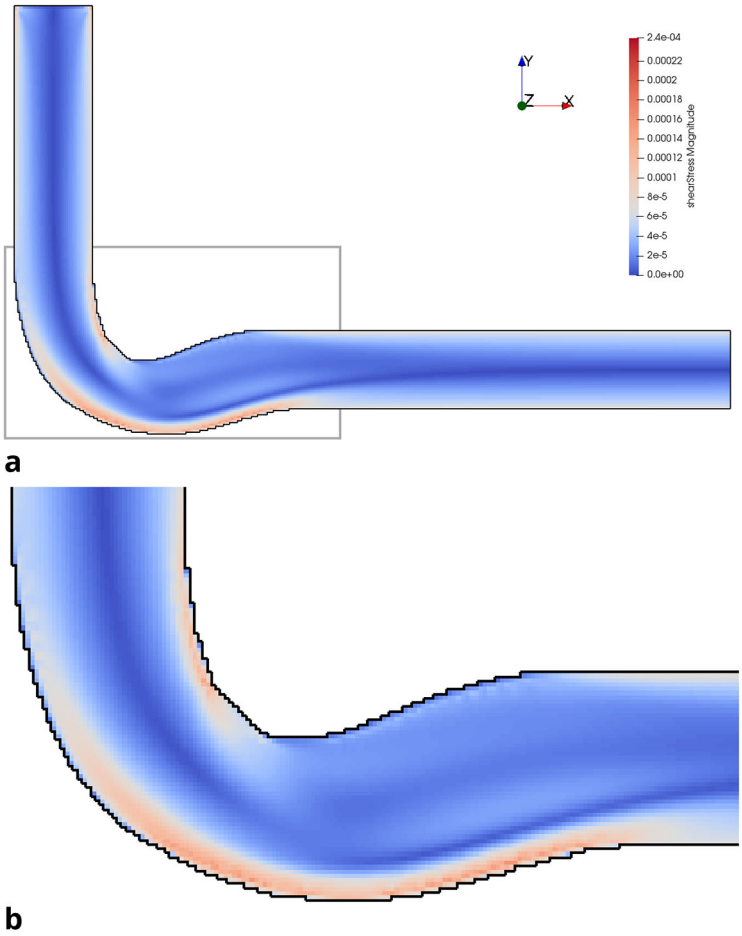

Figure 15. Shear stress in optimised 3D pipe elbow at *Re* = 200. (a) Full geometry. Grey box indicates area of detailed view in figure below. (b) Detail of geometry.

Table 6. Comparing pressure drop Δp at a given Reynolds number through the dedicatedly derived shape and the shape derived at *Re* = 40.

	Flow at Re	Shape optimised at Re					$\Delta p_{opt}/\Delta p_{Re=40}$
2D channel		40		200		500	
const. V	40	0.322		––		––	––
	200	0.122		0.130		––	1.065
	500	0.027		––		0.036	1.335
const. d	40	0.739		––		––	––
	200	0.452		0.472		––	1.045
	500	0.206		––		0.255	1.237
3D pipe		40	100	200	400		
const. d	40	0.902	––	––	––		––
	100	0.776	0.972	––	––		1.253
	200	0.746	––	0.943	––		1.265
	400	0.672	––	––	0.832		1.237

5. Conclusion

The aim of this research was to assess the potential pressure drop reduction by changing the fluid domain path without affecting its diameter at $Re \geq 40$. This was partly achieved by combining the existing heuristic optimality criterion with a further constraint of keeping the average diameter constant. Simulations conducted using this procedure revealed some limitations of the algorithm: Firstly, the cross section of 3D pipes deviated from the initial circular profile at $Re \geq 100$. Secondly, and more importantly, for any flow with $Re \geq 100$, 2D and 3D shapes optimised specifically for this Reynolds number resulted in a higher pressure drop than a reference shape derived at $Re = 40$. This behaviour was observed not only for shapes derived with a fixed average diameter, but also when the fluid volume was kept constant, as proposed by Wang et al.[6] and Park et al.[9] We concluded that the capability of the heuristic optimality criterion to optimise the investigated initial shapes is limited at $Re \geq 100$.

Future work should address several open questions. First, the physical mechanisms causing reduced performance at $Re \geq 100$ merit investigation—is the wall shear stress criterion insufficient at higher Reynolds numbers where inertial effects dominate? Alternative criteria (pressure-based or multi-objective optimization) could be explored. More importantly, the unexpected finding that shapes derived at $Re = 40$ outperform Reynolds-number-specific designs at $Re \geq 100$ opens an intriguing research direction: these geometries may also provide pressure drop reduction for turbulent flows at much higher Reynolds numbers. Many industrial applications—air ducts, fluid distributors, and heat exchangers—operate in the turbulent regime where direct simulation-based optimization becomes computationally prohibitive. If the transferability of low-Re derived geometries extends into the turbulent regime, the heuristic optimality criterion with the novel diameter constraint could offer a practical, computationally efficient design approach for industrial applications. Wang et al. successfully demonstrated such transfer in fluid distributor design; systematic investigation of this phenomenon, particularly with diameter-constrained optimization, represents a valuable avenue for future research with significant industrial relevance. Second, the method could be extended to other geometries (bifurcations, manifolds) and optimization objectives (bend angle optimization, cross-sectional shape preservation). Third, grid independence and experimental validation studies would support engineering applications and verify the reliability of the reshaping algorithm in preserving or modifying specific geometric features. Finally, the significant cross-section deformation observed in 3D pipes at high Reynolds numbers suggests additional geometric constraints may be needed to preserve desired cross-sectional profiles for manufacturing considerations.

While this study focuses on numerical validation through literature comparison, experimental validation would be valuable for engineering applications.

Data and software availability

Underlying data

Zenodo: Data for SEROS publication. https://doi.org/10.5281/zenodo.7788202

This project contains the following underlying data:

- rhobarInletAvg_analysis (Summary of achieved Pressure Drop Reduction (PDR) of all cases.)
- pre-processing-cases.zip (Directories containing the following files directly generated with SEROS.)
  - bestSeros (Iteration at PDR was highest.)
  - config2D_L.xml (Case configuration for creation of data.)
  - measurementsSeros0 (Fluid measurements taken at each reshaping iteration.)
  - plbLog.dat (Log file generated during simulation execution.)
  - rho*.ppm (Visualisation of fluid density fields at given iterations.)
  - vtk*.vti (Fluid field at highest PDR available for some cases.)
- 2D_L_Re*_PDR.txt (Identical with measurementsSeros0 for each 2D case.)
- 3D_L_Re*_PDR.txt (Identical with measurementsSeros0 for each 3D case.)

Data are available under the terms of the Creative Commons Attribution 4.0 International license (CC-BY 4.0)

Software availability

David Blacher. (2023). AIT-LKR/SEROS: First Release with full source code (v1.0-full-source-code). Zenodo. https://doi.org/10.5281/zenodo.7788368

The software is also available under a AGPL license here: https://github.com/AIT-LKR/SEROS

Acknowledgements

The authors would like to thank Stephan Jäger for his conceptual contributions towards the method and support in development of the software. Generative AI assistance: Claude Sonnet 4.5 was used to support drafting and language refinement of the revised manuscript; the authors reviewed and are responsible for all content.

References

1. Gersborg-Hansen A, Sigmund O, Haber RB: **Topology optimization of channel flow problems.** *Structural and Multidisciplinary Optimization.* Sep 2005; **30**(3): 181–192.
Publisher Full Text

2. Villanueva CH, Maute K: **CutFEM topology optimization of 3d laminar incompressible flow problems.** *Computer Methods in Applied Mechanics and Engineering.* jun 2017; **320**: 444–473.
Publisher Full Text

3. Borrvall T, Petersson J: **Topology optimization of fluids in stokes flow.** *International Journal for Numerical Methods in Fluids.* 2003; **41**(1): 77–107.
Publisher Full Text

4. Dilgen CB, Dilgen SB, Fuhrman DR, *et al.*: **Topology optimization of turbulent flows.** *Computer Methods in Applied Mechanics and Engineering.* 2018; **331**: 363–393. ISSN 0045-7825.
Publisher Full Text

5. Behrou R, Ranjan R, Guest JK: **Adaptive topology optimization for incompressible laminar flow problems with mass flow constraints.** *Computer Methods in Applied Mechanics and Engineering.* 2019; **346**: 612–641. ISSN 0045-7825.
Publisher Full Text

6. Wang L, Fan Y, Luo L: **Heuristic optimality criterion algorithm for shape design of fluid flow.** *Journal of Computational Physics.* oct 2010; **229**(20): 8031–8044.
Publisher Full Text

7. Wang L, Fan Y, Luo L: **Lattice boltzmann method for shape optimization of fluid distributor.** *Computers & Fluids.* may 2014; **94**: 49–57.
Publisher Full Text

8. Tarlet D, Fan Y, Luo L: **Design and mixing performance characterization of a mini-channel mixer with nature-inspired geometries.** *Chemical Engineering Research and Design.* dec 2020; **164**: 230–239.
Publisher Full Text

9. Park J, Safdari A, Kim KC: **Shape optimization of flow channels based on lattice boltzmann method.** *Journal of Mechanical Science and Technology.* jun 2018; **32**(6): 2619–2627.
Publisher Full Text

10. Tao M, Guo K, Huang Z, *et al.*: **A hybrid optimization method to design shapes of three-dimensional flow channels.** *Chemical Engineering Research and Design.* 08 2016; **114**.
Publisher Full Text

11. Latt J, Malaspinas O, Kontaxakis D, *et al.*: **Palabos: Parallel lattice boltzmann solver.** *Computers & Mathematics with Applications.* jan 2021;**81**: 334–350. ISSN 0898-1221.
Publisher Full Text

12. Succi S: *The lattice Boltzmann equation: for fluid dynamics and beyond.* Oxford university press. 2001.
Publisher Full Text

13. Latt J, Chopard B: **Lattice boltzmann method with regularized pre-collision distribution functions.** *Mathematics and Computers in Simulation.* Sep 2006; **72**(2-6): 165–168. ISSN 0378-4754.
Publisher Full Text

14. Blacher D: **Physical shape optimisation of channels and pipes to improve fluid flow.** *Diploma thesis, Technische Universität Wien.* 2021. reposiTUm.
Publisher Full Text

15. Goodman AW, Goodman G: **Generalizations of the theorems of pappus.** *The American Mathematical Monthly.* 1969; **76**(4): 355–366. ISSN 00029890.
PubMed Abstract | **Publisher Full Text**

16. Fuhrmann S, Kazhdan M, Goesele M: **Accurate isosurface interpolation with hermite data**. *2015 International Conference on 3D Vision.* oct 2015; 256–263. IEEE.
Publisher Full Text

Open Peer Review

Current Peer Review Status: ? ? ? ✓ ? ?

Version 2

Reviewer Report 05 May 2026

https://doi.org/10.21956/openreseurope.25194.r72105

© **2026 Filipeson Sozinando D.** This is an open access peer review report distributed under the terms of the Creative Commons Attribution License, which permits unrestricted use, distribution, and reproduction in any medium, provided the original work is properly cited.

✓ **Desejo Filipeson Sozinando**
Vaal University of Technology, Vanderbijlpark, South Africa

Most of the key issues raised in the initial review have been appropriately addresed in the revised version, in particular the method's performance at higher Reynolds numbers and the need for methodological clarity. The manuscript now presents improved technical clarity, alongside a more comprehensive discussion and well-defined future work. Minor issues remain but do not affect the overall scientific quality.

Competing Interests: No competing interests were disclosed.

Reviewer Expertise: Vibration Analysis, Fluid-Structure Interaction, Mathematical Modelling, FEA/CFD, Machine Learning.

I confirm that I have read this submission and believe that I have an appropriate level of expertise to confirm that it is of an acceptable scientific standard.

Reviewer Report 22 April 2026

https://doi.org/10.21956/openreseurope.25194.r72651

© **2026 Ali S.** This is an open access peer review report distributed under the terms of the Creative Commons Attribution License, which permits unrestricted use, distribution, and reproduction in any medium, provided the original work is properly cited.

? **Sarmad A Ali**
University of Babylon, Babylon, Iraq

1- Revise the title to clearly reflect the scientific novelty (constant diameter constraint) and highlight the key finding related to Re = 40.

2- Improve the abstract by clearly stating the research gap and problem, including study limitations (especially at high Reynolds numbers), and avoiding overgeneralization to turbulent flows.
3- Update the introduction with recent references (≥50% from the last 5 years) and better emphasize the originality and research gap.
4- Strengthen the introduction by adding real industrial application examples to justify the importance of the study.
5- Expand the description of the Lattice Boltzmann Method (LBM), including justification for its use over conventional CFD, with discussion of its advantages and limitations.
6- Clearly state the model assumptions (Newtonian fluid, laminar flow, isothermal conditions) and discuss their impact on generalizability.
7- Provide stronger justification for the selection of numerical parameters (velocity, viscosity, relaxation time, adaptation time).
8- Conduct a grid independence study to ensure the reliability and robustness of the results.
9- Perform a sensitivity analysis for key parameters (e.g., f_e , f_s) and evaluate their effect on convergence and stability.
10- Improve the mathematical model presentation by adding deeper physical interpretation of equations and ensuring consistency of symbols.
11- Clarify the optimization algorithm (erosion/sedimentation), justify parameter choices, and define convergence criteria more rigorously.
12- Enhance the results section with detailed physical analysis (e.g., shear stress distribution, flow patterns, vortex structures).
13- Provide a clear scientific explanation for the superior performance at Re = 40 and the reduced effectiveness at Re ≥ 100.
14- Support results with quantitative comparisons to previous studies and/or alternative optimization methods.
15- Expand the discussion to include analysis of non-convergence and sensitivity to initial geometry.
16- Address cross-sectional deformation in 3D cases and discuss its implications for practical/industrial applications.
17- Explicitly state the methodological limitations within the discussion section.
18- Revise the conclusions to avoid unsupported generalizations and ensure all claims are directly supported by results.
19- Strengthen the future work section with specific directions (e.g., experimental validation, turbulent flow modeling, industrial applications).
20- Update and improve the references by including recent studies in CFD and LBM, and ensure consistency in formatting, along with improving the clarity and quality of figures and tables.

Is the work clearly and accurately presented and does it cite the current literature?

Partly

Is the study design appropriate and does the work have academic merit?

Yes

Are sufficient details of methods and analysis provided to allow replication by others?

Yes

If applicable, is the statistical analysis and its interpretation appropriate?

Partly

Are all the source data underlying the results available to ensure full reproducibility?
Partly

Are the conclusions drawn adequately supported by the results?
Yes

Competing Interests: No competing interests were disclosed.

I confirm that I have read this submission and believe that I have an appropriate level of expertise to confirm that it is of an acceptable scientific standard, however I have significant reservations, as outlined above.

Version 1

Reviewer Report 14 August 2024

https://doi.org/10.21956/openreseurope.17217.r37318

© **2024 Mousavi S.** This is an open access peer review report distributed under the terms of the Creative Commons Attribution License, which permits unrestricted use, distribution, and reproduction in any medium, provided the original work is properly cited.

?

S Mahmood Mousavi
[1] Seoul National University (Ringgold ID: 26725), Gwanak-gu, Seoul, South Korea
[2] Texas State University, San Marco, Texas, USA

1-The numerical simulations conducted using the Lattice Boltzmann method should be described in detail, including the range of Reynolds numbers tested and any limitations or assumptions made.

2- The method showed less effectiveness at higher Reynolds numbers. This is a significant limitation as many real-world applications operate in these regimes.

3-There seems to be a lack of comparative analysis with other methods. It would be beneficial to see how this method stacks up against traditional approaches under similar conditions.

Is the work clearly and accurately presented and does it cite the current literature?
Partly

Is the study design appropriate and does the work have academic merit?
Yes

Are sufficient details of methods and analysis provided to allow replication by others?

Partly

If applicable, is the statistical analysis and its interpretation appropriate?
Not applicable

Are all the source data underlying the results available to ensure full reproducibility?
Yes

Are the conclusions drawn adequately supported by the results?
Yes

Competing Interests: No competing interests were disclosed.

Reviewer Expertise: Aerodynamic and reacting flow

I confirm that I have read this submission and believe that I have an appropriate level of expertise to confirm that it is of an acceptable scientific standard, however I have significant reservations, as outlined above.

Reviewer Report 14 August 2024

https://doi.org/10.21956/openreseurope.17217.r38577

© 2024 Filipeson Sozinando D. This is an open access peer review report distributed under the terms of the Creative Commons Attribution License, which permits unrestricted use, distribution, and reproduction in any medium, provided the original work is properly cited.

?

Desejo Filipeson Sozinando
Vaal University of Technology, Vanderbijlpark, South Africa

The study aimed to minimize internal pressure drop in pipes and enhance the energy efficiency of fluid flow applications. The study proposed combining the heuristic optimization approach with a new geometrical constraint to assess pressure drop reduction solely by modifying the flow path while keeping the average diameter constant. This adds a novel aspect to the research, expanding on existing optimization techniques. The study conducts numerical simulations using the Lattice Boltzmann method with Reynolds numbers ranging from 40 to 500. However, the limited capability of the heuristic criterion to derive improved shapes with a minimum pressure drop is limited at Re $\geq$ 100 to achieving improvements which do not necessarily represent the optimal solution.

General comments
The study appears to have academic merit, and the idea of the article is very interesting, but the authors have some shortcomings. The response and the suggested recommendation would define the acceptance of the manuscript.

Specific Comments:
In order to have a better understanding of the manuscript, some aspects need to be clarified.

1. **Highlighted of section 1:**
   - The manuscript has about 17 references. Using 2023 as a baseline, the manuscript cited ten relevant works older than five years. In other words, 58% of the literature is older than five years. I recommend more than 50% of the current literature (not older than five years).
2. **Highlighted of section 2.1:**
   - How does the lattice Boltzmann method discretize the Navier-Stokes equations? What is the advantage in terms of accuracy and efficiency of the results over the traditional CFD method?
3. **Highlighted of section 2.2:**
   - Can you please justify the reason for the initialization of the velocity of the resultant new fluid nodes with zero after erosion? And how does this initialisation influence the fluid-solid interface's behaviour during reshaping?
4. **Highlighted of section 3.1:**
   - May the authors state one or two alternative ways of calculating wall-neighbouring nodes fractions (f_s and f_e) affected by sedimentation and erosion, and what influence do they have on the outcomes of reshaping?
   - In what ways does the strain rate, which guides the reshaping algorithm, differ between viscous and inviscid fluid domains? How does this difference impact the effectiveness of the algorithm?
   - What role does viscosity play in determining the stability and convergence of the reshaping algorithm, especially in relation to the recommended fraction of affected nodes by Wang et al.? and how were these affected nodes determined?
5. **Highlighted of section 3.3:**
   - I would advise not including numbering in Figure 5, since the arrows already indicate the algorithm's articulation.
6. **Highlighted of section 5:**
   - In conclusion, it is stated that "the limited capability of the heuristic criterion to derive improved shapes with a minimum pressure drop is limited at Re $\geq$ 100 to achieving improvements which do not necessarily represent the optimal solution." I advise the author to recommend future research to address these limitations and improve the effectiveness of the reshaping algorithm for complex fluid flow scenarios. I also advise authors to recommend future work to validate or verify how reliable and accurate the reshaping algorithm is, especially in preserving desired geometric features.

Is the work clearly and accurately presented and does it cite the current literature?
Partly

Is the study design appropriate and does the work have academic merit?
Yes

Are sufficient details of methods and analysis provided to allow replication by others?
Partly

If applicable, is the statistical analysis and its interpretation appropriate?
Yes

Are all the source data underlying the results available to ensure full reproducibility?

Yes

Are the conclusions drawn adequately supported by the results?
Partly

Competing Interests: No competing interests were disclosed.

Reviewer Expertise: Vibration Analysis, Fluid Structure Interaction, Fracture Mechanics

I confirm that I have read this submission and believe that I have an appropriate level of expertise to confirm that it is of an acceptable scientific standard, however I have significant reservations, as outlined above.

Reviewer Report 19 March 2024

https://doi.org/10.21956/openreseurope.17217.r38568

© 2024 Ferroudji H. This is an open access peer review report distributed under the terms of the Creative Commons Attribution License, which permits unrestricted use, distribution, and reproduction in any medium, provided the original work is properly cited.

?

Hicham Ferroudji
Boumerdes University, Boumerdes, Algeria

The manuscript addressed the flow through pipes with a constant diameter using the heuristic optimality criterion.

It is an interesting manuscript, however, the following would improve the quality of the paper:

1. More details about the numerical model.

2. Comparison with experimental data from the literature to validate and test the accuracy of the model.

3. I would recommend to state clearly the originality of the work.

Is the work clearly and accurately presented and does it cite the current literature?
Yes

Is the study design appropriate and does the work have academic merit?
Yes

Are sufficient details of methods and analysis provided to allow replication by others?
Partly

If applicable, is the statistical analysis and its interpretation appropriate?

I cannot comment. A qualified statistician is required.

Are all the source data underlying the results available to ensure full reproducibility?
Partly

Are the conclusions drawn adequately supported by the results?
Partly

Competing Interests: No competing interests were disclosed.

Reviewer Expertise: Numerical modeling of internal fluid flows

I confirm that I have read this submission and believe that I have an appropriate level of expertise to confirm that it is of an acceptable scientific standard, however I have significant reservations, as outlined above.

Reviewer Report 19 March 2024

https://doi.org/10.21956/openreseurope.17217.r37322

© 2024 Roy S. This is an open access peer review report distributed under the terms of the Creative Commons Attribution License, which permits unrestricted use, distribution, and reproduction in any medium, provided the original work is properly cited.

?

Somnath Roy
Department of Mechanical Engineering, Indian Institute of Technology Kharagpur, Kharagpur, West Bengal, India

This article presents an interesting study for optimization of duct shapes. However, the major comment is regarding not presenting validation and grid independence study for the LBM method. The authors should add it in the revised manuscript.

Also, can this method be extended on bend angle optimization as well as on higher Re flows?

Is the work clearly and accurately presented and does it cite the current literature?
Yes

Is the study design appropriate and does the work have academic merit?
Yes

Are sufficient details of methods and analysis provided to allow replication by others?
Partly

If applicable, is the statistical analysis and its interpretation appropriate?
Yes

Are all the source data underlying the results available to ensure full reproducibility?
Partly

Are the conclusions drawn adequately supported by the results?
Yes

Competing Interests: No competing interests were disclosed.

Reviewer Expertise: Computational Fluid Dynamics

I confirm that I have read this submission and believe that I have an appropriate level of expertise to confirm that it is of an acceptable scientific standard, however I have significant reservations, as outlined above.

Reviewer Report 21 February 2024

https://doi.org/10.21956/openreseurope.17217.r37314

© 2024 Rehman S. This is an open access peer review report distributed under the terms of the Creative Commons Attribution License, which permits unrestricted use, distribution, and reproduction in any medium, provided the original work is properly cited.

?

Sohail Rehman
Islamia College Peshawar, Peshawar, Pakistan

The main observations are listed below. The acceptance of the manuscript would depend on the revision. The author needs to provide a point by point response or provide a rebuttal.

1. *How did you get the convergence of the numerical method LBM ?.*
2. *The authors have not explained, what type fluid is selected, what is motivation for selecting this fluid model, and what are the real world applications of this fluid under the conditions studied in this paper.*
3. *Provide mathematical expression for fluid volume.*
4. *As the study considers the constitutive modeling of a virtual fluid dynamics phenomena without validating the results from any physical experimental data. While modeling such virtual fluid dynamics phenomena, the authors take many assumptions to formulate the mathematical model, which may not be real and practical. Therefore, further explanation about physical configuration of problem should be included and the results should be discussed with relation to physical parameters involved in the model. The authors should also explain the physical situation is being modeled in the manuscript.*
5. *Explain the physical significance of boundary conditions and the reasoning behind their transformations.*
6. *Detailed comparison of the current results with results from other literature or commercial (CFD) codes are preferred to show the advantages and disadvantages of the presented model?*
7. *Please enrich the introduction section with related studies.*

References
1. Hashim, Rehman S, Mohamed Tag Eldin E, Bafakeeh O, et al.: Coupled energy and mass transport for non-Newtonian nanofluid flow through non-parallel vertical enclosure. *Ain Shams Engineering Journal*. 2023; **14** (8). Publisher Full Text
2. Rehman S, Hashim, Alqahtani S, Alshehery S: Modeling a non-Newtonian nanofluid flow between intersecting planes with slip mechanism. *Continuum Mechanics and Thermodynamics*. 2023; **35** (1): 61-80 Publisher Full Text
3. Boujelbene M, Rehman S, Hashim, Alqahtani S, et al.: Optimizing thermal characteristics and entropy degradation with the role of nanofluid flow configuration through an inclined channel. *Alexandria Engineering Journal*. 2023; **69**: 85-107 Publisher Full Text

Is the work clearly and accurately presented and does it cite the current literature?
Partly

Is the study design appropriate and does the work have academic merit?
Yes

Are sufficient details of methods and analysis provided to allow replication by others?
Partly

If applicable, is the statistical analysis and its interpretation appropriate?
I cannot comment. A qualified statistician is required.

Are all the source data underlying the results available to ensure full reproducibility?
Yes

Are the conclusions drawn adequately supported by the results?
Partly

Competing Interests: No competing interests were disclosed.

Reviewer Expertise: Fluid dynamics, Channel flow, Mathematical modeling

I confirm that I have read this submission and believe that I have an appropriate level of expertise to confirm that it is of an acceptable scientific standard, however I have significant reservations, as outlined above.